Angle dependent light scattering by gold nanospheres

2016 J. Phys.: Conf. Ser. 682 012018

(http://iopscience.iop.org/1742-6596/682/1/012018)

Angle dependent light scattering by gold nanospheres

J X Wang[1], A M Nilsson[1], D L A Fernandes[2] and G A Niklasson[1]

[1] Division of Solid State Physics, Department of Engineering Sciences, The Å ngström Laboratory, Uppsala University, P. O. Box 534, SE−751 21 Uppsala, Sweden
[2] Division of Physical Chemistry, Department of Chemistry, The Å ngström Laboratory, Uppsala University, P. O. Box 534, SE−751 21 Uppsala, Sweden

E−mail: Junxin.Wang@angstrom.uu.se

Abstract. Gold nanocrystals exhibit unique optical properties in enhanced light absorption and scattering owing to their extremely large scattering/absorption cross−sections and large electric field enhancements generated by localized surface plasmon resonance. In this work, the optical properties of gold nanospheres with diameters of 60 nm and 200 nm with remarkable uniformity in size were studied both numerically and experimentally. The total transmittance and reflectance as well as the angle−resolved light scattering intensities of the gold nanospheres were measured. The absorption and scattering coefficients were obtained by fitting the experimental data to the two−flux theory and were in qualitative agreement with single−scattering calculations using the Mie theory.

1. Introduction

Metallic nanocrystals have been receiving extensive attention for applications in optical and optoelectronic devices, and in solar energy technologies because of their extremely large scattering/absorption cross−sections and large electric field enhancements generated by localized surface plasmon resonance (LSPR). LSPR stems from the collective oscillations of conduction−band electrons, endowing noble metal nanocrystals with unique optical properties, *i.e.*, their LSPR wavelengths can be tailored from the visible to infrared regions by synthetically varying their shape and size [1]. Among them, gold nanospheres (NSs) are one of the most attractive plasmonic materials owing to their superior chemical and thermal stability, easy preparation by wet−chemistry approaches, and perfect geometrical symmetry. So far, a number of investigations have been published on plasmonic scattering enhancement on gold nanoparticles [2,3]. These studies focused mainly on the characterization of the absorption and scattering of gold nanoparticles with different shapes and sizes. However, wavelength and angle−resolved light scattering on gold nanoparticles has seldom been reported. In fact, the wavelength and angular dependent light scattering is one of the most critical issues for understanding how light propagates and interacts with the nanoparticles in the scattering layer. A thorough understanding of the spatial light scattering intensity distribution plays an essential role for controlling light scattering, which is highly desirable for further advancing photonic and display techniques such as solar cells, photodetectors, and LEDs [4–6].

In this paper, monodispersed gold nanospheres with diameters of 60 nm (NS60) and 200 nm (NS200) were investigated experimentally in terms of their extinction, total and diffuse reflectance and

transmittance. The absorption and scattering cross section of gold nanospheres were numerically explored by Mie theory as well as by fitting the experimental results to two–flux theory. Wavelength and angle–resolved light scattering properties on NS60 and NS200 samples were also investigated.

2. Experimental methods

Gold nanospheres – Gold nanosphere samples of two different sizes were obtained from NanoSeedz Ltd. (Hong Kong SAR, China) as non–standard products. As informed by the manufacturer, the gold nanospheres sample was prepared by a seed–mediated growth approach modified from their previously reported works [7].

Physical techniques – Scanning electron microscopy (SEM) imaging was conducted on an FEI Quanta 400 FEG microscope operating at 20 kV.

Optical measurements – Extinction spectra of gold nanospheres in water solution were measured in the spectral range from 300 nm to 1000 nm using a Perkin-Elmer Lambda 900 ultraviolet/visible/near-infrared spectrophotometer using 1 cm thick quartz cuvettes. The extinction value represents the optical density (OD), which equals the logarithm of (1/transmittance). Total transmittance T_{tot} and reflectance R_{tot}, as well as diffuse transmittance T_{dif} and reflectance R_{dif} were measured in the same Lambda 900 spectrophotometer. The spectrophotometer was equipped with a spectralon coated integrating sphere from LabSphere. Regular transmittance, T_{reg} and specular reflectance R_{spe}, were derived by subtracting the diffuse components T_{dif} and R_{dif} from the total components T_{tot} and R_{tot}. For the transmittance and reflectance measurements, the gold nanospheres sample in water solution was sandwiched between two sealed microscope slides (75 × 25 × 1 mm) with a gap of 50 μm. The refractive index of the glass n_g is close to 1.5.

Wavelength and angle–resolved scattering measurements – The measurement system [14] consists of a 250 W tungsten–halogen lamp with a stabilized *dc* power supply, a monochromator (SP–401), two gratings with blaze wavelength of 0.75 μm and 2.0μm, an off–axis parabolic aluminum mirror from Optical Surfaces Ltd, with an off–axis distance of 80 mm and a focal length of 410 mm. The detector is a silicon diode in the spectral response region from 300 nm to 1100 nm. Lock–in technique is used to monitor the signal from the detector (EG&G model 7260). The sample is centrally mounted and illuminated, the detector with an integrating sphere can be positioned at various angles from 0° to 180° to collect the scattered light that allows angle–resolved measurements to be taken.

3. Theroy

Mie scattering theory – The electrodynamic response of particles of spherical shape can be analytically and effectively solved with Mie theory in a classical electromagnetic framework [8]. In this work, our MATLAB code is based on the program in the appendix of the book by Bohren and Huffman [9]. We compute the scattering (C_{sca}), absorption (C_{abs}) and extinction (C_{ext}) cross sections divided by the volume of single nanosphere. The refractive index of surrounding water is set as 1.33.

Two flux theory – Two–flux models [10] offer a description of the optics of materials exhibiting diffuse light scattering. In detail, light scattering materials are modeled as a slab with thickness *d* in which diffuse light I_d is propagating in the forward direction and diffuse light J_d in the reverse direction [11]. The scattering and absorption coefficients are denoted S and K. The extinction coefficient is the sum of S and K. In the independent scattering approximation, S and K are related to the scattering and absorption cross sections [12] by:

$$S = \frac{fC_{sca}}{V} = \frac{fC_{sca}}{\frac{4}{3}\pi a^3} \quad (1)$$

$$K = \frac{fC_{abs}}{V} = \frac{fC_{abs}}{\frac{4}{3}\pi a^3} \quad (2)$$

where f is the volume fraction and a is the radius of the nanospheres. In two−flux theory, the Kubelka−Munk approximation [13] for the transmittance and reflectance, denoted as T_{KM} and R_{KM}, represent the total transmittance and reflectance for a layer on a transparent background and are given by:

$$T_{KM} = \frac{b(1-R_g)}{(a-R_g)\sinh(bSd) + b\cosh(bSd)} \tag{3}$$

$$R_{KM} = \frac{1-R_g[a-b\coth(bSd)]}{a-R_g+b\coth(bSd)} \tag{4}$$

where R_g is the total reflectance from the background, which is the backside glass/air interface in our case. The parameters a and b in equation (3) and (4) are given in terms of scattering and absorption coefficients, with $a = 1+K/S$ and $b = (a^2-1)^{0.5}$.

This Kubelka-Munk approximation neglects the front surface reflection, and in order to take it into account we obtain [13]:

$$T = \frac{(1-R_c)T_{KM}}{1-R_jR_{KM}} \tag{5}$$

$$R = R_c + \frac{(1-R_c)(1-R_j)R_{KM}}{1-R_jR_{KM}} \tag{6}$$

where R_c is the reflectance of collimated light incident at the front air/glass surface. R_j denotes the reflectance of partially diffuse light from the nanoparticles, impinging onto the front glass/air interface.

4. Results and Discussions

Scanning electron microscopy (SEM) imaging (figure 1a and c) shows that the obtained gold NSs possess spherical shapes and smooth surfaces. The NS60 sample possesses a nearly spherical geometry with an average diameter measured to 60 ± 5 nm. The surface morphology of NS200 is a bit rough, and the average diameter of the spheres was measured to 200 ± 15 nm.

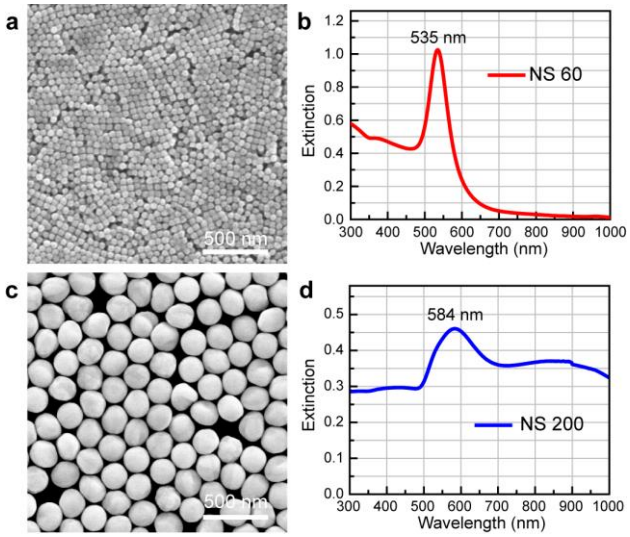

Figure 1. SEM (a,c) and extinction spectra (b,d) of gold nanosphere samples with average diameters of 60 ± 5 nm (a,b) and 200 ± 15 nm (c,d). The particle concentrations and volume fractions are $1.7\cdot10^{10}$ particles/mL, $1.9\cdot10^{-6}$ and $6.5\cdot10^{9}$ particles/mL, $2.8\cdot10^{-5}$ for NS60 and NS200, respectively.

The rough surfaces of gold nanocrystals severely affect their scattering intensities and profiles, therefore gold nanocrystals with nearly spherical shapes and smooth surfaces with narrow size distributions are highly sought after. The extinction spectra of NS60 and NS200 samples were

acquired in water solution in figure 1b and d. The maximum extinction wavelength of NS60 peaks at 535 nm corresponding to the dipolar plasmon mode. It red shifts to around 800 nm in NS200 sample. A quadrupole plasmon mode appeared around 560 nm for NS200 sample. Peak broadening is clearly observed owing to increasing radiative losses for the gold NSs with larger sizes [15]

In order to obtain the scattering and absorption coefficients from two−flux theory, the gold nanosphere solutions were sandwiched between two sealed glass slides with a gap around 50 μm. The total, diffuse and regular transmittance as well as the total, diffuse and specular reflectance of these samples are shown in figure 2. For the NS60 sample, the total transmittance curve and the regular transmittance curve almost overlap, indicating the main transmittance change comes from the absorption of the nanospheres. The transmittance drops below 350 nm due to the absorption of the glass slides. The diffuse transmittance is almost negligible in NS60, a weak peak centered at 560 nm can be observed owing to the diffuse scattering of the nanoparticles. In regard to the reflectance of NS60 in figure 2c, the specular reflectance mainly corresponds to the reflectance from the glass slide, which is around 8%. The valley near 535 nm corresponds to the strong absorption of the dipolar plasmon mode of NS60. The diffuse reflectance peak at 560 nm indicates the backward scattering of NS60 sample. Compared to NS60 sample, the contribution from the diffuse part is higher in NS200 sample as shown in figure 2b. In figure 2d, the specular reflectance is almost a flat curve at 8%, and the valley around 560 nm can hardly been seen due to the weak quadrupole plasmon absorption of NS200. The diffuse reflectance is significant and originates from backward scattering from the NS200 sample.

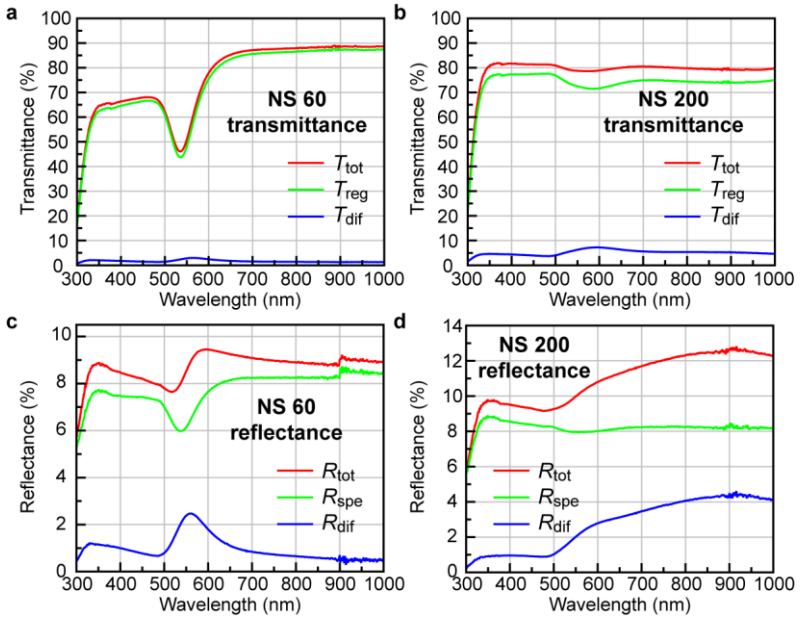

Figure 2. Measured total, regular and diffuse transmittance (upper row) and total, specular and diffuse reflectance (bottom row) of NS60 (a, c) and NS200 (b, d) samples. The particle concentrations and volume fractions are $6.7{\cdot}10^{11}$ particles/mL, $7.6{\cdot}10^{-5}$ and $2.6{\cdot}10^{11}$ particles/mL, $1.1{\cdot}10^{-3}$ for NS60 and NS200, respectively.

Figure 3 compares the scattering, absorption and extinction coefficients per volume when derived from Mie scattering theory or from experimental data using the two−flux theory for NS60 and NS200 samples. The results for the NS60 sample are in good agreement with the Mie theory, indicating a very good morphology and size distribution of the NS60 sample. In addition the low volume fraction of $7.6{\cdot}10^{-5}$ diminishes the interactions between particles so that the results agree well with the Mie theory which deals with a single nanoparticle. The results for the NS200 sample calculated from two−flux

theory show discrepancies from the Mie result. We speculate that agglomeration of particles may have occurred and resulted in the red shift of the whole spectrum.

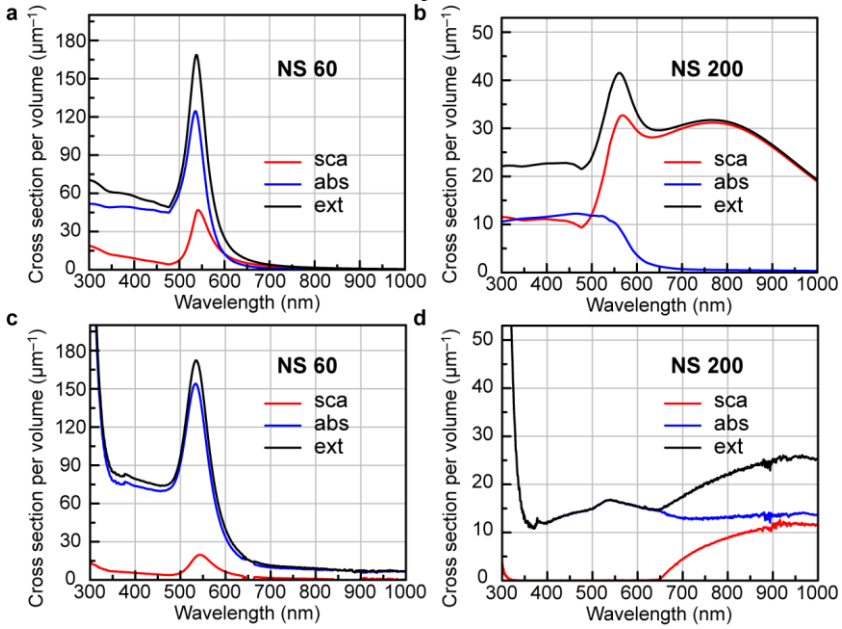

Figure 3. Scattering, absorption and extinction cross section per volume for NS60 (a) and NS200 (b) samples calculated using Mie theory. Scattering, absorption and extinction cross section per volume of NS60 (c) and NS200 (d) calculated from measured *T*, *R* results in figure 2 using two–flux theory.

In figure 4, the scattering intensity is presented as a function of wavelength and angle for the NS60 and NS200 samples. The regular component of the transmitted light dominates for angles from 0° to 4° in our angle–resolved setup. As proved by both numerical simulation and experimental measurement in figure 2 and 3, the diffuse scattering from NS60 sample is relatively low compared to its absorption. A weak diffuse scattering peak at 560 nm can be observed in figure 2a and figure 3c, while the scattering intensities are very low at 500 nm and 600 nm. The large–angle scattering observed at 300 nm and 400 nm may arise from a weak Rayleigh scattering component. In contrast to NS60, NS200 shows stronger scattering intensities, even at wavelengths larger than 500 nm. This is reasonable since the diffuse transmittance on the NS200 is significant at wavelengths larger than 500 nm as shown in figure 2.

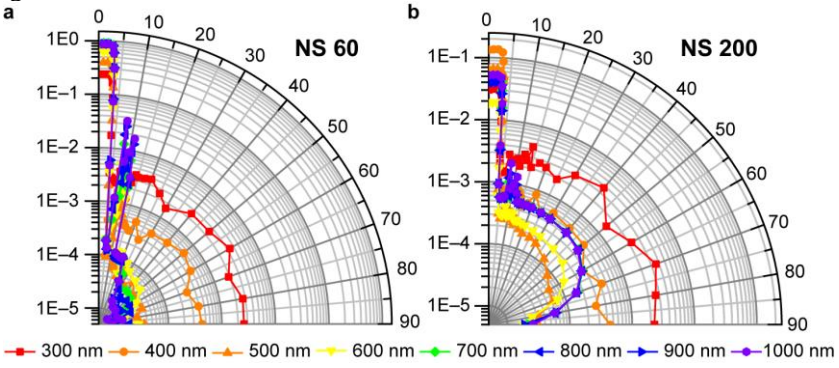

Figure 4. Wavelength and angle–resolved light scattering measurement conducted in the transmittance regime of NS60 (a) and NS200 (b) samples.

5. Conclusions

The extinction, reflectance and transmittance have been measured on suspensions of gold nanospheres with diameters of 60 nm and 200 nm. The scattering and absorption cross sections have been derived based on fitting of experimental data to two–flux theory. For the 60 nm particles the results are consistent with the Mie scattering theory. Wavelength and angle–resolved scattering measurements were carried out, and a strong wavelength and angular dependence of light scattering for the particles was established.

Acknowledgements

This paper was presented at the INERA Conference "Light in Nanoscience and Nanotechnology" in Hissar, Bulgaria, October 19–22, 2015. The conference is part of the INERA REGPOT project of the Institute of Solid State Physics, Bulgarian Academy of Sciences. Chemical gold nanosphere samples of two different sizes were obtained from NanoSeedz Ltd. (Hong Kong SAR, China). Scanning electron microscopy images were performed by Qifeng Ruan.

References

[1] Ni W H, Kou X S, Yang Z and Wang J F 2008 *ACS Nano* 2 677–686
[2] Baek S –W, Park G, Noh J, Cho C, Lee C –H, Seo M –K, Song H and Lee J –Y 2014 *ACS Nano* **8** 3302–3312
[3] Fang C H, Jia H L, Chang S, Ruan Q F, Wang P, Chen T and Wang J F 2014 *Energy Environ. Sci.* **7** 3431–3438
[4] Yang M, Fu Z P, Lin F and Zhu X 2011 *Opt. Express* **19** A763–771
[5] Montgomery G P 1988 *J. Opt. Soc. Am. B* **5** 774–784
[6] David A 2013 *J. Display Technol.* **9** 301–316
[7] Ruan Q F, Shao L, Shu Y W, Wang J F and Wu H K 2014 *Adv. Opt. Mater.* **2** 65–73
[8] Mie G 1908 *Annalen der Physik* **330** 377–445
[9] Bohren C F and Huffman D R 1983 *Absorption and Scattering of Light by Small Particles* (New York: Wiley)
[10] Vargas W E 1998 *Appl. Opt.* **25** 1122–1128
[11] Barrios D, Vergaz R, Sanchez–Pena J M, Granqvist C G and Niklasson G A 2013 *Sol. Energy Mater. Sol. Cells* **111** 115–122
[12] Niklasson G A and Eriksson T S 1988 *Proc. SPIE* **1016** 89–99
[13] Kubelka P 1948 *J. Opt. Soc. Am.* **38** 448–457
[14] Nostell P and Roos A 1999 *Rev. Sci. Inst.* **70** 2481–2494
[15] Rodríguez–Fernández J, Pérez–Juste J, Abajo F J G d and Liz–Marzán L M 2006 *Langmuir* **22** 7007–7010